Supplementary Information

Synthesis of Carbon Nitride in Potassium Hydroxide Molten Salt for Efficient Uranium Extraction from Radioactive Wastewater

Shuang Liu [a,b], Junhan Luo [a], Daniel-James Maguire [c], Liyuan Zheng [d], Zhe Wang [a,*], Yuexiang Lu [a,*]

[a]Institute of Nuclear and New Energy Technology, Tsinghua University, Beijing 100084, China

[b]Nuclear Research Institute for Future Technology and Policy, Seoul National University, Seoul 08826, Republic of Korea

[c]Department of Earth Sciences, University of Cambridge, Cambridge CB23EQ, United Kingdom

[d]The MOE Key Laboratory of Resources and Environmental System Optimization, College of Environmental Science and Engineering, North China Electric Power University, Beijing 102206, PR China

[*] Corresponding author: Tel: +86-010-89796068. E-mail: wang2023@tsinghua.edu.cn (Zhe Wang) & luyuexiang@mail.tsinghua.edu.cn (Yuexiang Lu)

Supporting Texts

Experimental

XPA-7 photochemical reactor (purchased from Nanjing Xujiang Machine-Electronic Plant, China) was utilized in the photocatalytic reaction. As shown in Scheme S1, the Xe lamp was placed vertically in the center of a platform, surrounding is quartz cooling trape, which can bring away the heat caused by the lamp and meanwhile permit thorough transmission of light ranging from ultraviolet to visible range. The optical filters vertically lie between the reactors and lamp. The reactors are placed outside of the platform, parallel to the tube lamp. The distance between the lamp and reactors is about 10 cm. The tube reactors are also made in quartz. Multiple magnetic agitators are installed just under the tube reactors. For the dark reaction, the light was kept turning off and main reaction box was closed to create dark reaction environment.

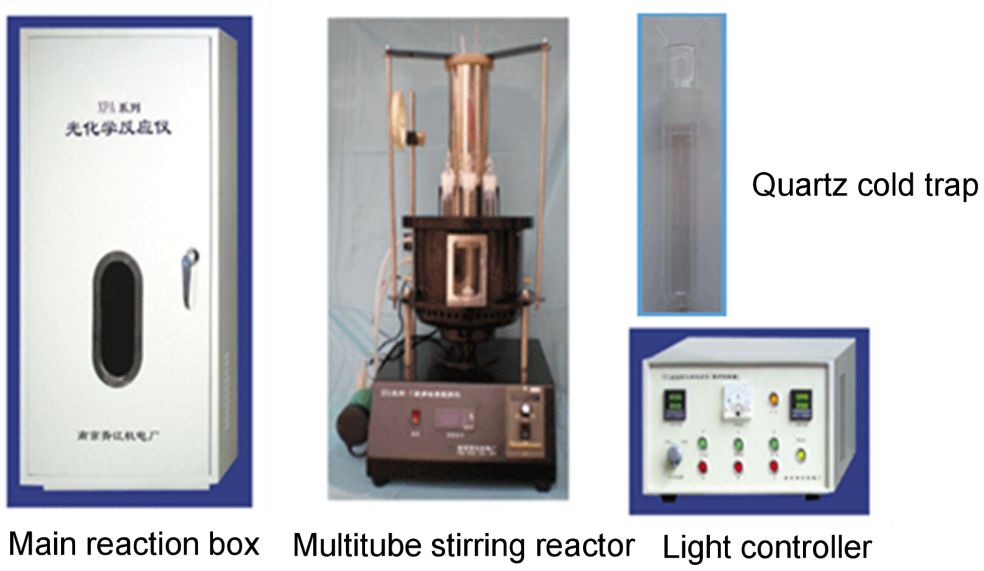

Scheme S1. XPA-7 photocatalytic reactor images

Characterization

X-ray diffraction (XRD) patterns were obtained by a D/max-2400 X-ray powder diffractometer with Cu-Kα radiation (Rigaku, Japan), and Fourier-transform infrared (FTIR) spectroscopies were measured by Nexus 470 FT-IR spectrometer (Nicolet, US). The ultraviolet-visible spectrophotometry (UV-vis) was obtained by UV-3600 (Shimadzu, Japan) and X-ray photoelectron spectroscopy (XPS) was conducted with a Vario EL III instrument (Elementar, Germany) with a mono Al-Kα X-ray source (1361 eV). NMR (JNM-ECZ600R spectrometer with MAS frequency of 12 kHz and cross polarization magic angle spinning) was conducted for molecular structure characterization. Fluorescence spectroscopy (FL) was utilized for the structural characterization of the K-CN-w on a FluoroMax-4 (HORIBA, Japan). The morphologies were recorded by scanning electron microscopy (SEM) on a LEO 1530 (ZEISS, Germany). Specific surface areas and pore size were determined by the Brunauer-Emmett-Teller (BET) method. The concentration of uranium was measured by the Arsenazo III method with a 721-type ZF-1 spectrophotometer (Shanghai Baoshan Gucun Photoelectric Instrument Factory, China) at 652 nm.

Supporting Figures

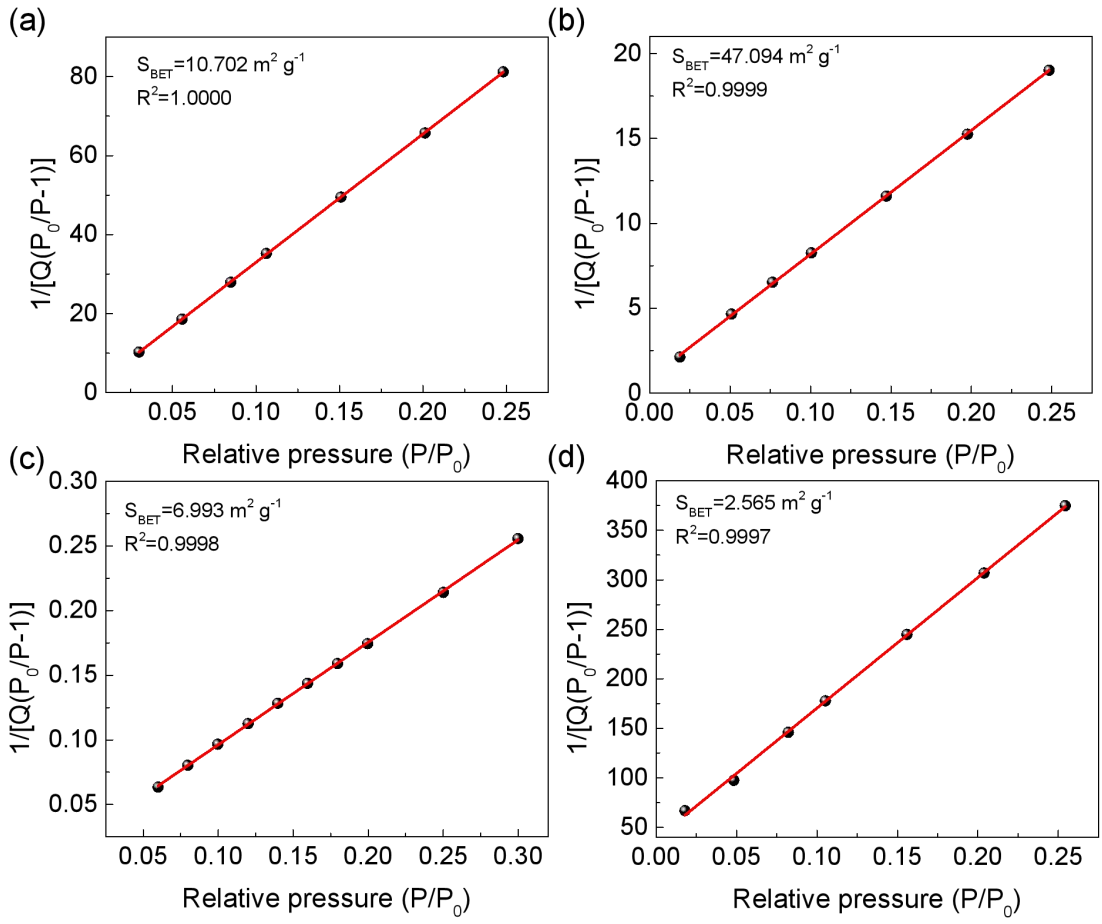

Figure S1. BET plots and linear fitting of g-C_3N_4, K-CN-70, K-CN-80 and K-CN-90, respectively.

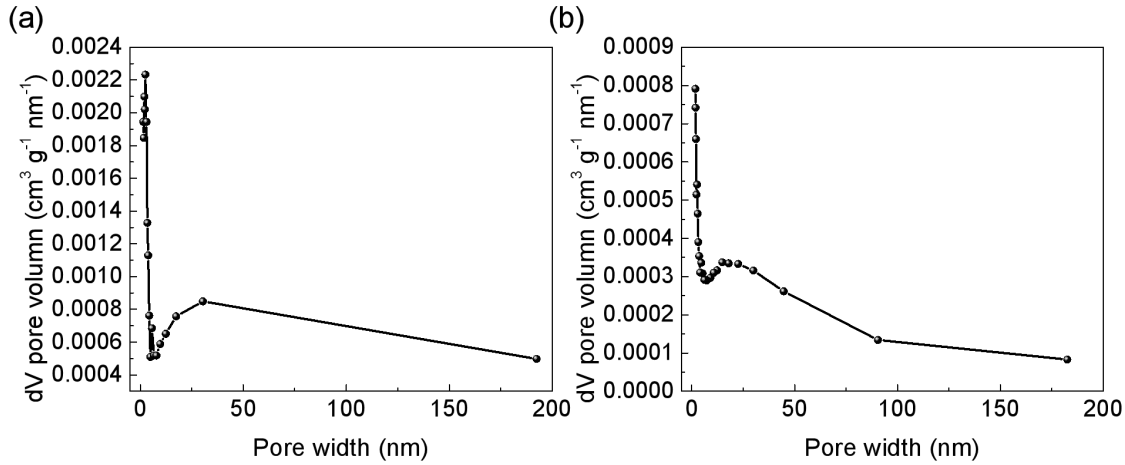

Figure S2. Pore size distribution of g-C_3N_4 and K-CN-80.

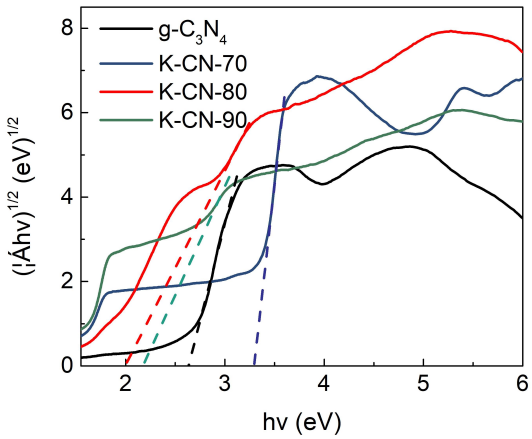

Figure S3. Tauc Plot of g-C_3N_4, K-CN-70, K-CN-80 and K-CN-90, respectively.

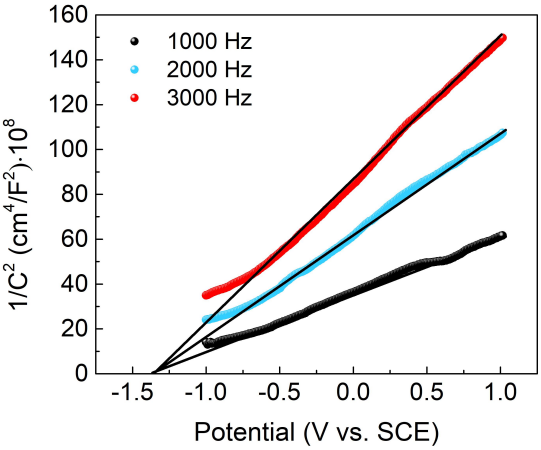

Figure S4. Mott-Schottky plots of g-C_3N_4 at 1000, 2000 and 3000 Hz.

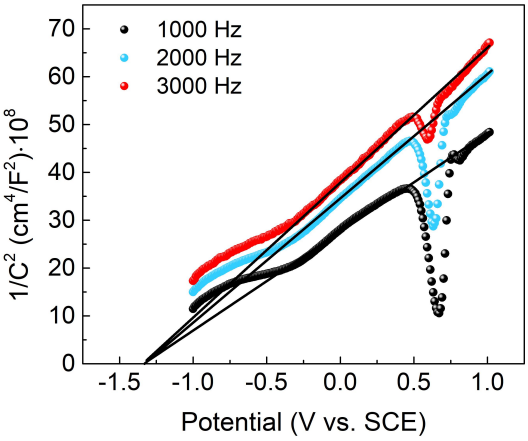

Figure S5. Mott-Schottky plots of K-CN-70 at 1000, 2000 and 3000 Hz.

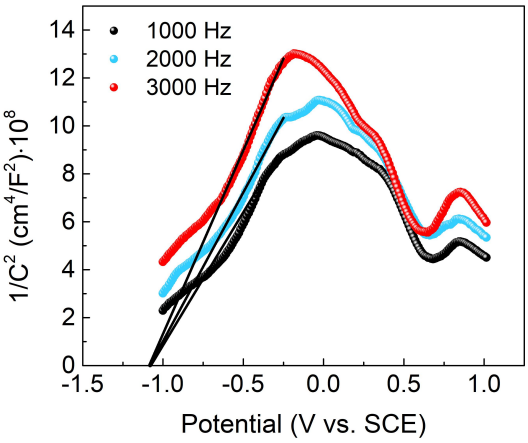

Figure S6. Mott-Schottky plots of K-CN-80 at 1000, 2000 and 3000 Hz.

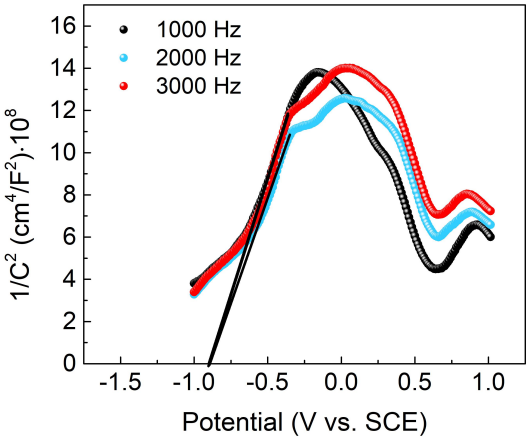

Figure S7. Mott-Schottky plots of K-CN-90 at 1000, 2000 and 3000 Hz.

Supporting Tables

Table S1. FWHM of the various peak components from the spectra in Figure 4.

Component	Peaks	Energy (eV)	FWHM (eV)			
			$g\text{-}C_3N_4$	K-CN-70	K-CN-80	K-CN-90
C	C1	284.6	1.2	1.2	1.3	1.2
	C2	286.5	1.5	1.2	1.3	1.9
	C3	288	1.1	1.5	1.5	1.2
N	N1	398.4	1.0	1.3	1.2	1.2
	N2	399.7	2.7	2.5	2.2	2.2
	N3	400.4	1.3	1.4	1.5	1.5
K	K1	292.6	-	1.3	1.3	1.4
	K2	295.3	-	1.2	1.2	1.6

Table S2. Apparent reaction rate constant(k) of $g\text{-}C_3N_4$, K-CN-70, K-CN-80, K-CN-90

Materials	Zero-crossing	
	Apparent reaction rate constant（min^{-1}）	R^2
$g\text{-}C_3N_4$	0.0006	0.6008
K-CN-70	0.0008	0.7926
K-CN-80	0.0039	0.9917
K-CN-90	0.0013	0.8968

Table S3. The comparison of photocatalytic extraction performance of different carbon nitride materials.

Materials	Initial U(VI) concentration ($mg\ L^{-1}$)	Capacity ($mg\ g^{-1}$)	Kinetics (min^{-1})	Improvement on reaction rate	pH	Ref
g-C_3N_4/TiO_2-1	10	25	0.2222	56.97	5	(Liu et al., 2021)
MoS_2/g-C_3N_4	21.2	18	-	-	4.5	(Huang et al., 2022)
CN/AC-0.3	98.5	46.3	0.07164	70	5	(Li et al., 2022)
CCN-500	40	80	0.132	2.5	5	(Wu et al., 2023)
CNBr0.1	40	80	0.083	2.2	5	(Xue et al., 2022)
K-CN-80	200.2	163.1	0.0039	6.6	4	This work